Supplementary Information

The effect of the oxidation level of graphene oxide substrate on in-situ growth of COF-300

Ying Quan [a,b], Yizhou Yang [b], Qinfu Liu *[a], Karl Börjesson *[b]

[a] School of Geosciences and Surveying Engineering, China University of Mining and Technology (Beijing), 100083 Beijing, China

[b] Department of Chemistry and Molecular Biology, University of Gothenburg, Medicinaregatan 19, 41390 Gothenburg, Sweden

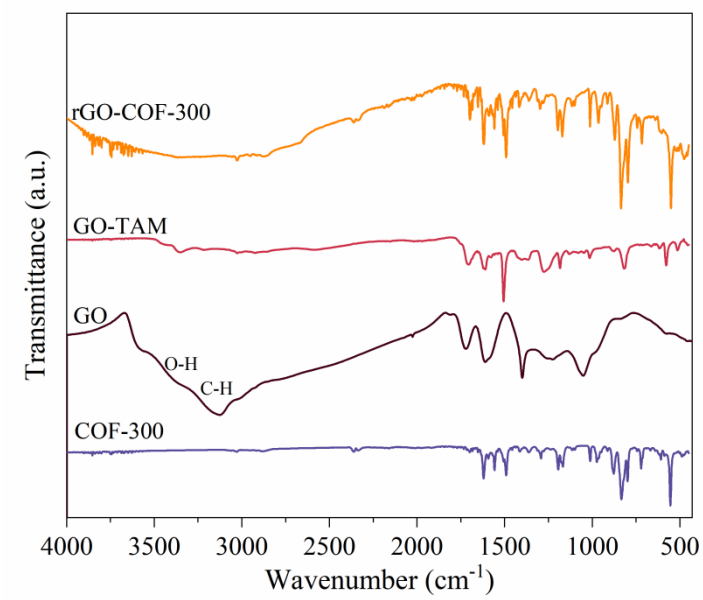

Fig. S1 Full FT-IR spectra of GO, GO-TAM, rGO-COF-300 and COF-300.

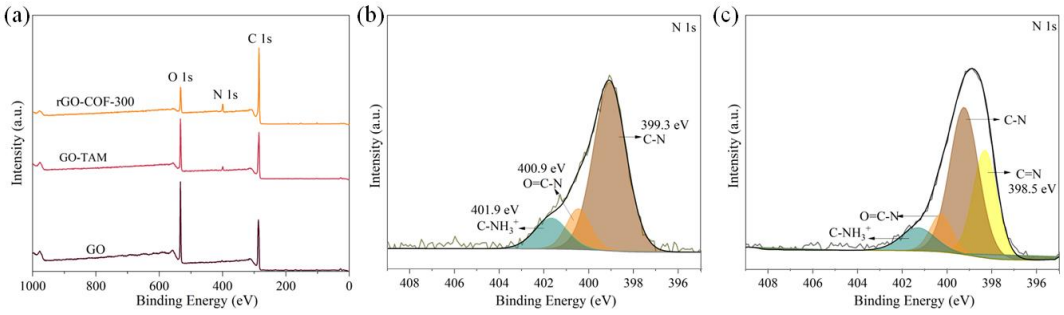

Fig. S2 (a) Wide scanning XPS spectra of GO, GO-TAM and rGO-COF-300 and (b) high-resolution N 1s spectra of (a) GO-TAM and (b) rGO-COF-300.

Fig. S3 The digital photo of the TAM stirred for 3 h at 60 °C under the same acid conditions but without the GO dispersion.

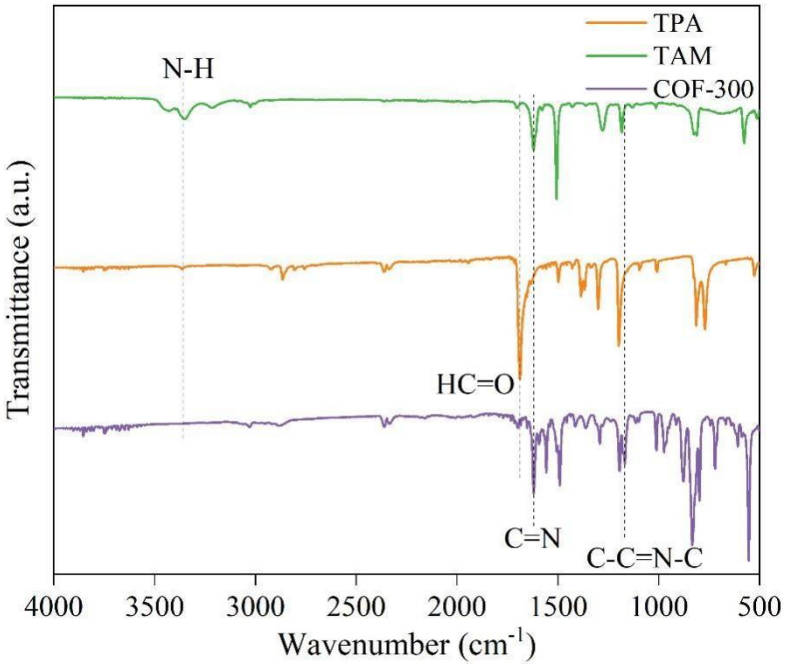

Fig. S4 FT-IR spectra of TPA monomer, TAM monomer and COF-300.

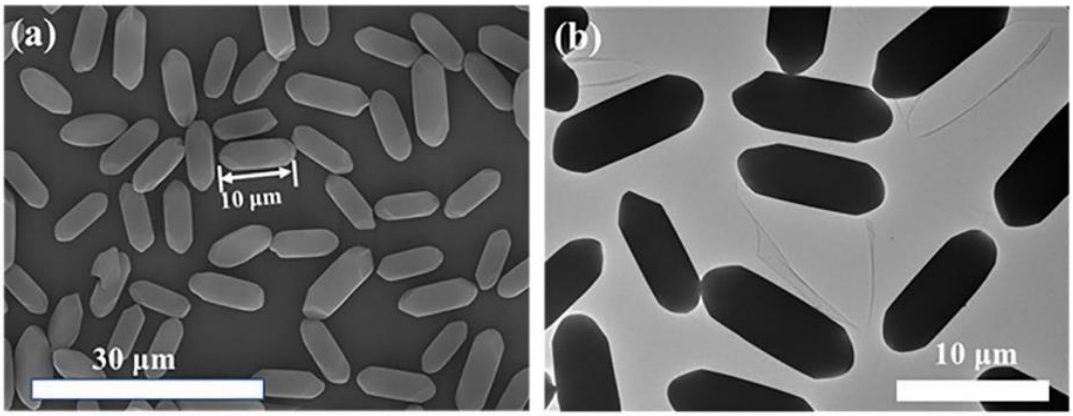

Fig. S5. (a) SEM image and (b) TEM image of single COF-300.

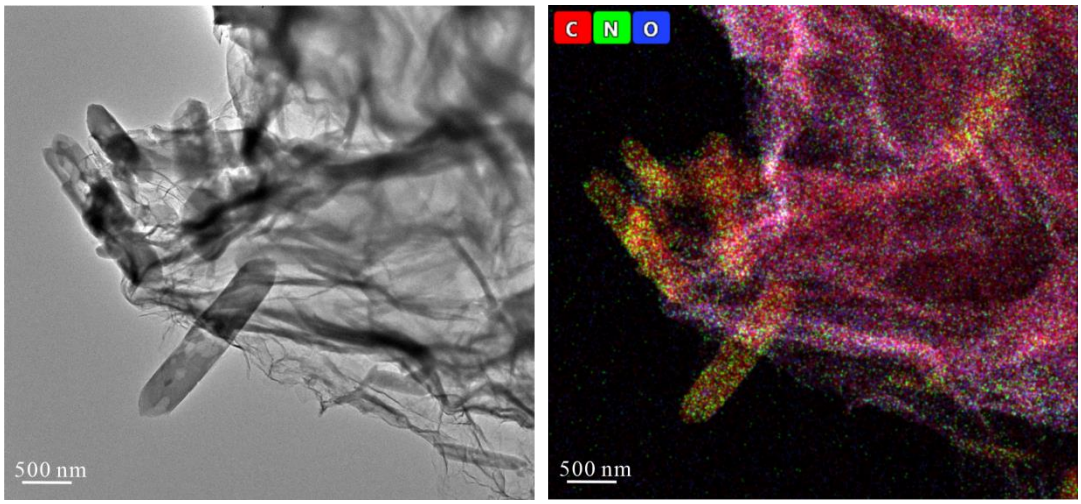

Fig. S6. TEM image and the corresponding EDS mapping of rGO-COF-300.

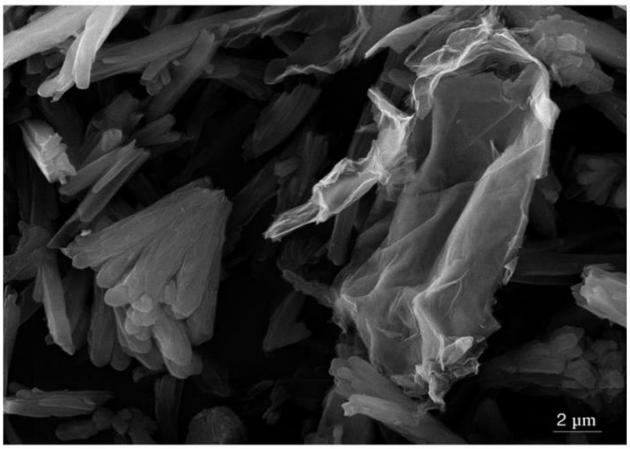

Fig. S7. SEM image of the BlankG-COF-300.

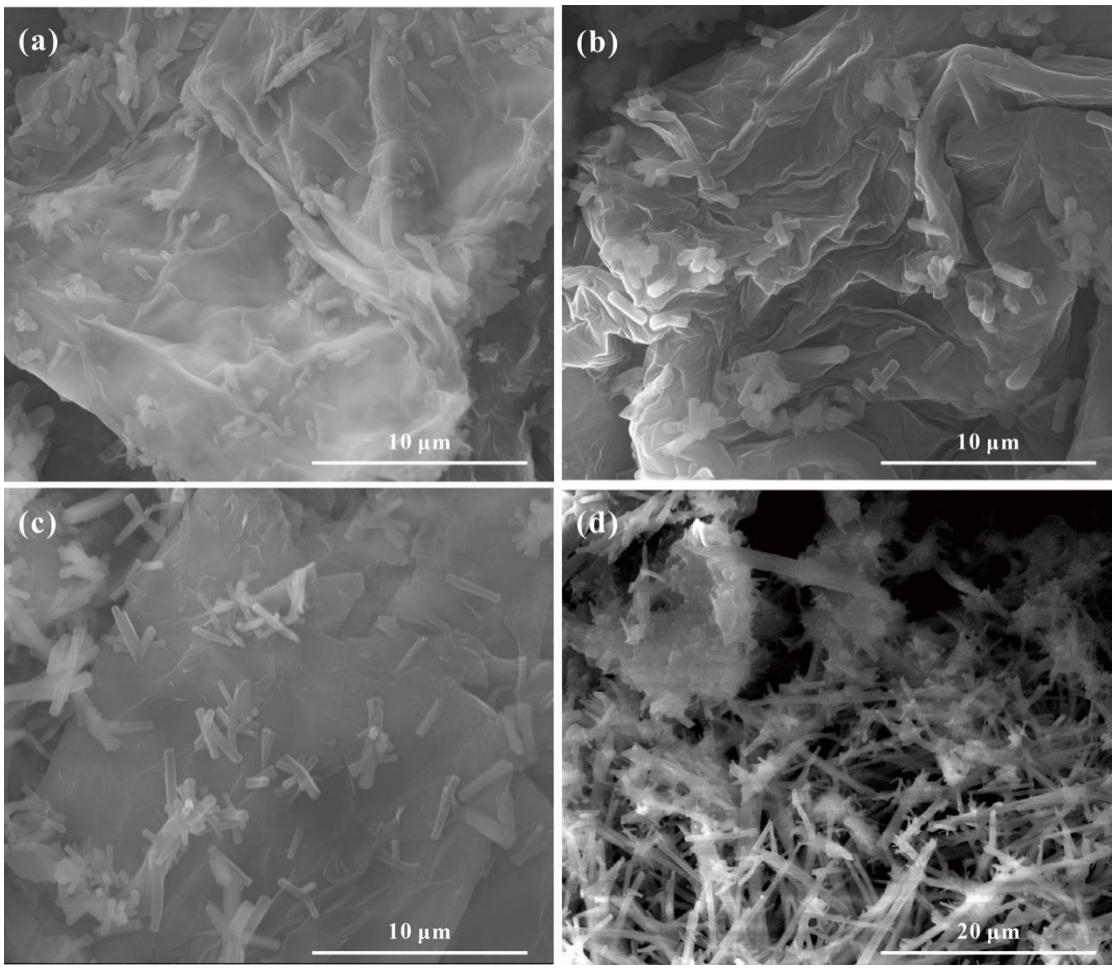

Fig. S8. SEM images of (a) 30 rGO-COF-300 (GO concentration, 30 mg/mL), (b) 20 rGO-COF-300 (GO concentration, 20 mg/mL), (c) 10 rGO-COF-300 (GO concentration, 10 mg/mL) and (d) 1 rGO-COF-300 (GO concentration, 1 mg/mL).

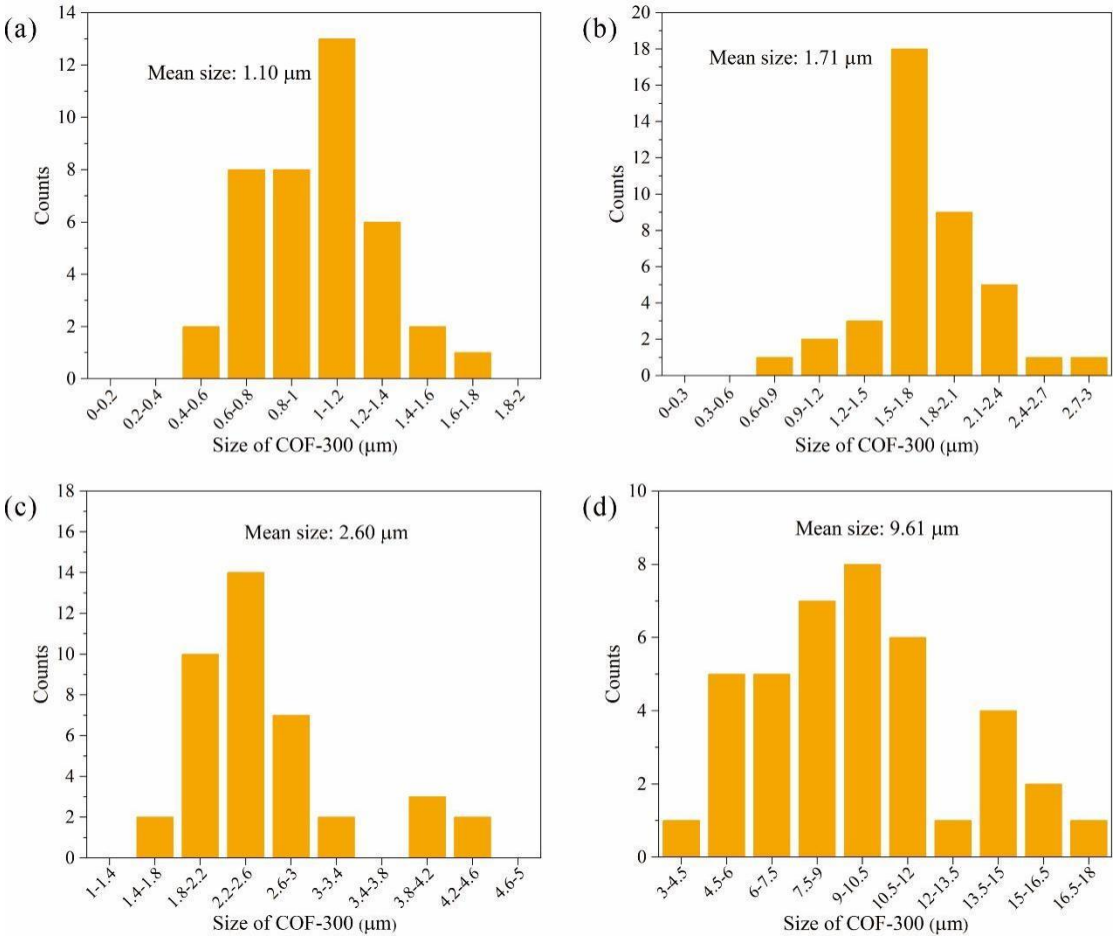

Fig. S9. Size distribution histograms of the COF-300 by SEM images, (a) 30 rGO-COF-300, (b) 20 rGO-COF-300, (c) 10 rGO-COF-300 and (d) 1 rGO-COF-300.

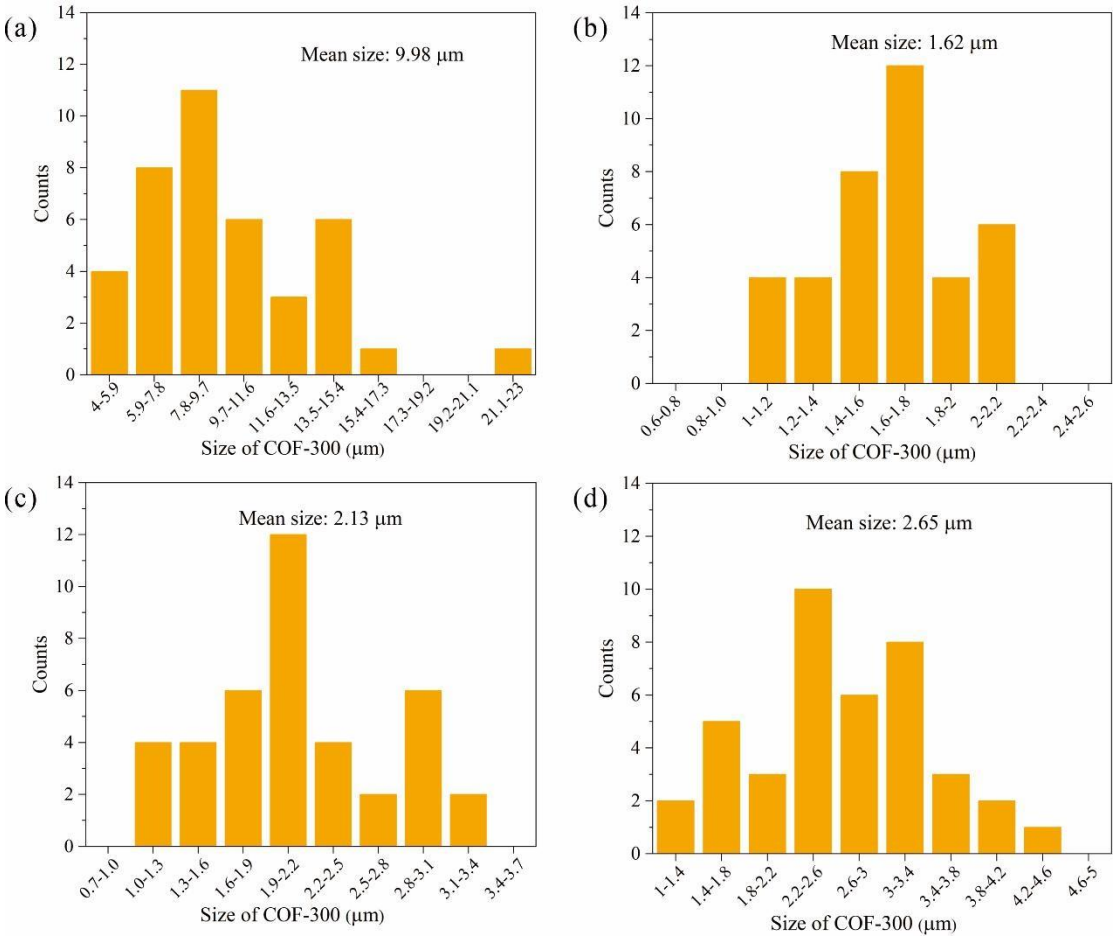

Fig. S10. Size distribution histograms of the COF-300 by SEM images, (a) pure COF-300, (b) rGO (Source 1)-COF-300, (c) rGO (Source 2)-COF-300 and (d) rGO (Source 3)-COF-300.

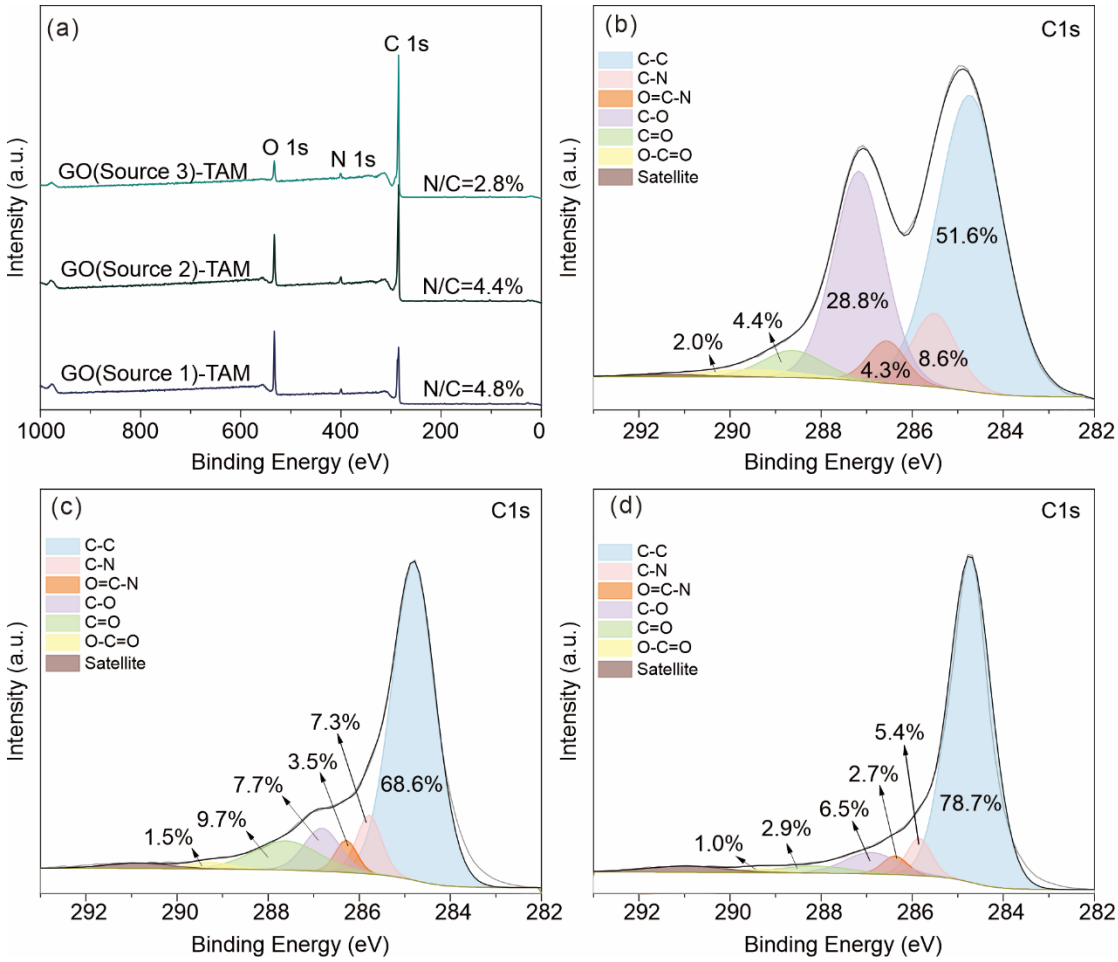

Fig. S11. (a) Wide scanning XPS spectra of GO-TAM, and high-resolution C 1s spectra of (b) GO (Source 1)-TAM, (c) GO (Source 2)-TAM, (d) GO (Source 3)-TAM.

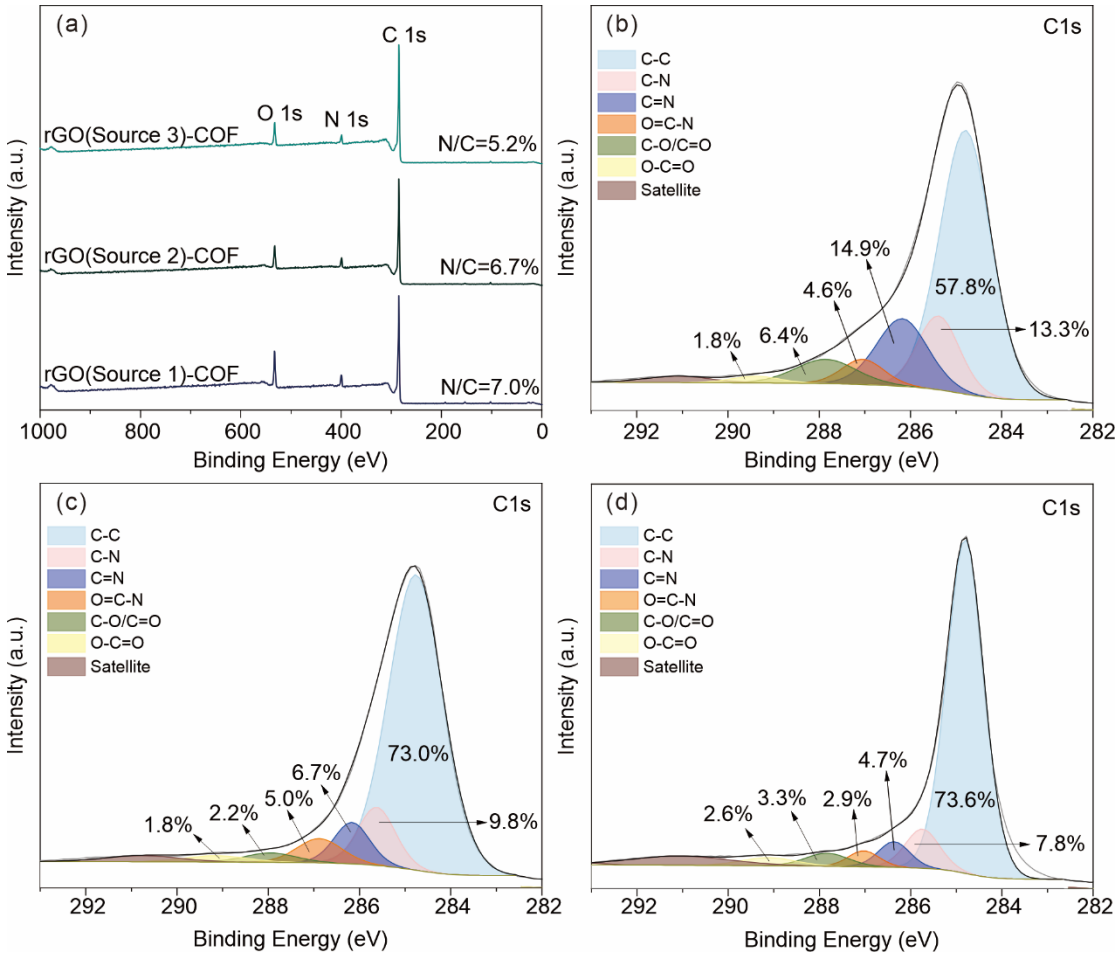

Fig. S12. (a) Wide scanning XPS spectra of rGO-COF-300, and high-resolution C 1s spectra of (b) rGO (Source 1)-COF-300, (c) rGO (Source 2)-COF-300 and (d) rGO (Source 3)-COF-300.

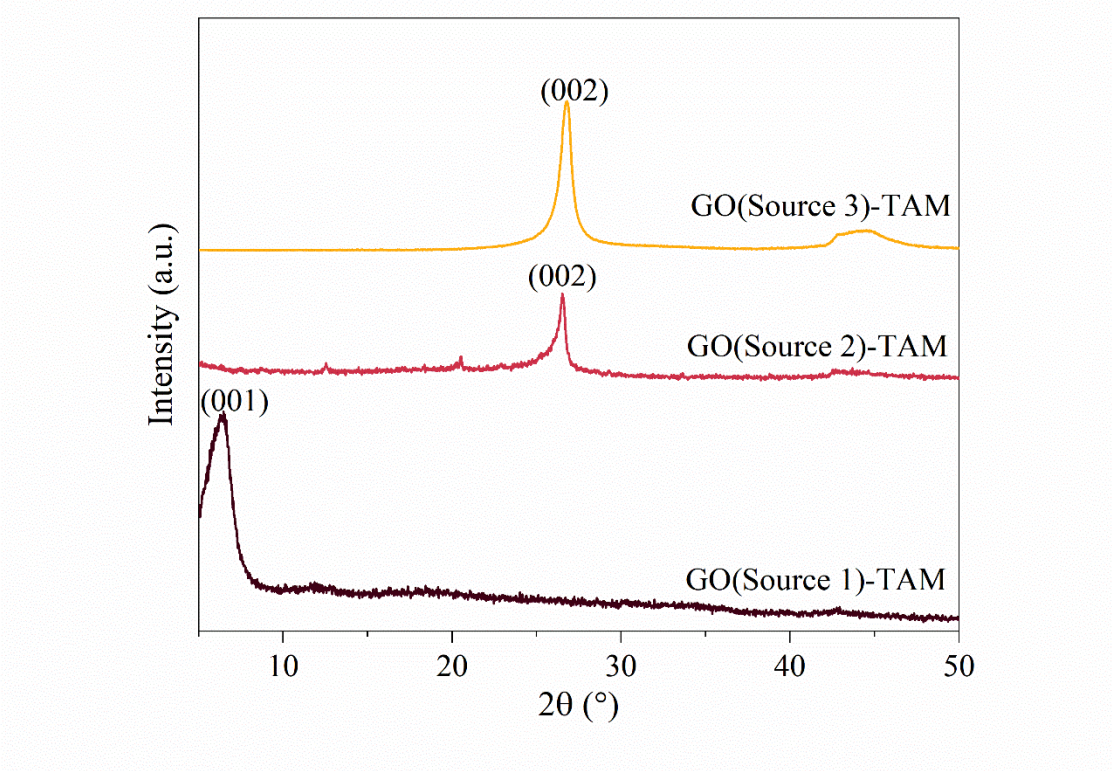

Fig. S13. The XRD patterns of GO (Source 1)-TAM, GO (Source 2)-TAM and GO (Source 3)-TAM.

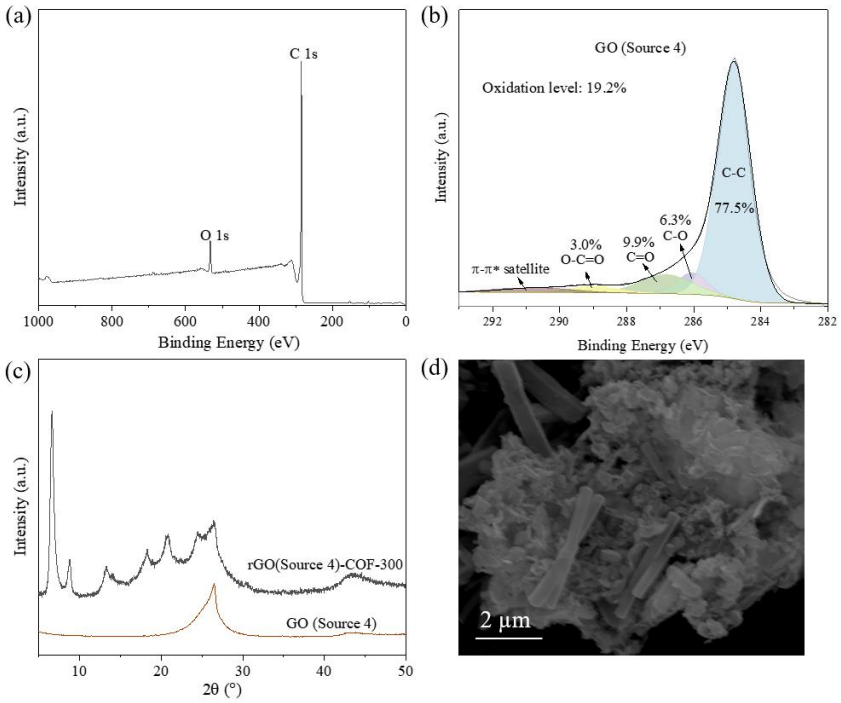

Fig. S14. (a) Wide scanning XPS spectra and (b) high-resolution C 1s spectra of GO (Source 4) substrate, (c) XRD patterns of GO (Source 4) substrate and rGO (Source 4)-COF-300 composite, and (d) SEM image of rGO (Source 4)-COF-300.

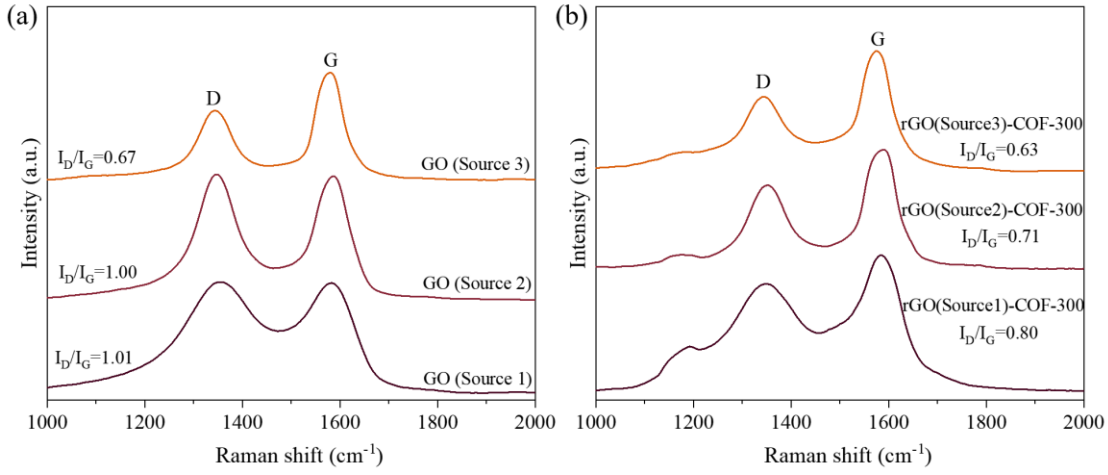

Fig. S15. Raman spectra of (a) GO and (b) rGO-COF-300 composites.

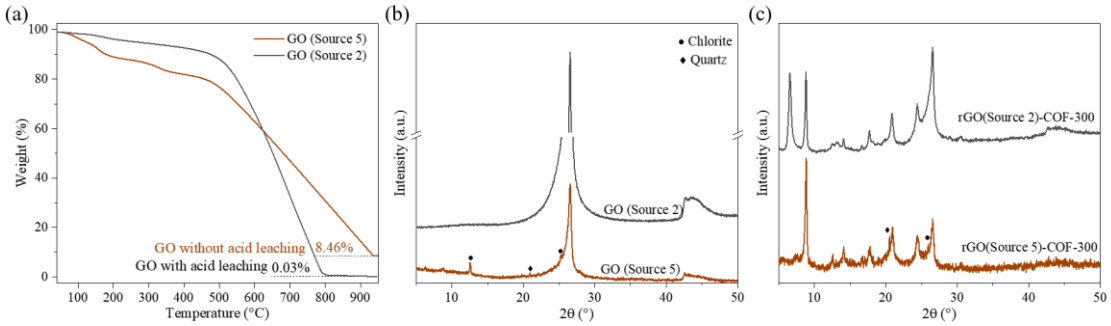

Fig. S16. (a) TG plots and (b) XRD patterns of the GO (Source 5) and its precursor GO (Source 2), (c) XRD patterns of rGO (Source 5)-COF-300 and rGO (Source 2)-COF-300.

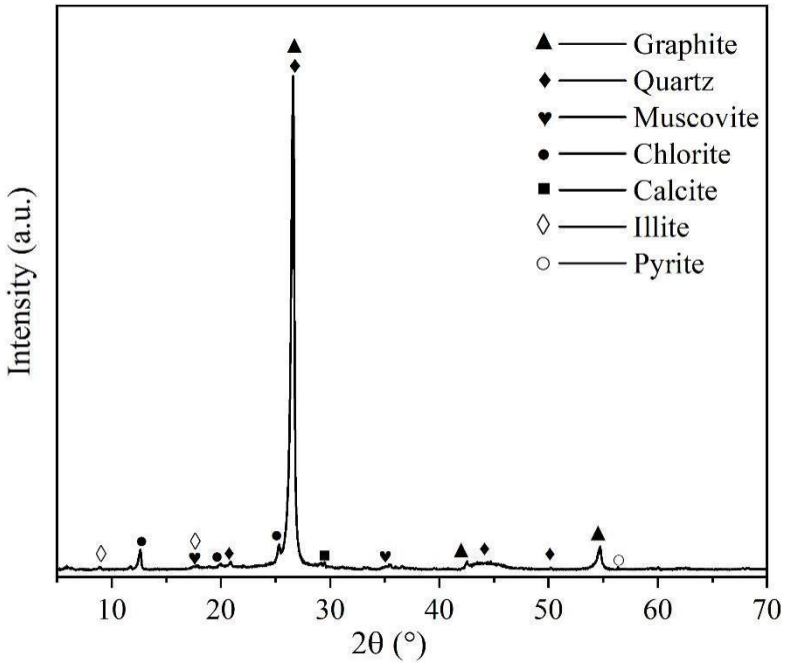

Fig. S17. XRD pattern of the natural coaly graphite from Lutang mining area.

Table S1. Elemental analysis of GO-TAM and rGO-COF-300 from the EDS data in Figure 3. The nitrogen content in COF-300 ($C_{33}H_{30}N_4O_2$) is 10.9 %. Thus, suggesting a COF-300 loading of about 37 % in the rGO-COF-300.

Samples	C, wt%	N, wt%	TAM loading, wt%	COF-300 loading, wt%
GO-TAM	80.4	1.8	12.5	-
rGO-COF-300	84.4	4.0	-	36.9